JCB Article

Regulation of cytochrome *c* oxidase activity by c-Src in osteoclasts

Tsuyoshi Miyazaki,[1,2,3] Lynn Neff,[2] Sakae Tanaka,[3] William C. Horne,[1,2] and Roland Baron[1,2]

[1]Department of Cell Biology and [2]Department of Orthopaedics and Rehabilitation, Yale University School of Medicine, New Haven, CT 06520
[3]Department of Orthopaedic Surgery, Faculty of Medicine, The University of Tokyo, Tokyo 113-0033, Japan

The function of the nonreceptor tyrosine kinase c-Src as a plasma membrane–associated molecular effector of a variety of extracellular stimuli is well known. Here, we show that c-Src is also present within mitochondria, where it phosphorylates cytochrome *c* oxidase (Cox). Deleting the c-*src* gene reduces Cox activity, and this inhibitory effect is restored by expressing exogenous c-Src. Furthermore, reducing endogenous Src kinase activity down-regulates Cox activity, whereas activating Src has the opposite effect. Src-induced Cox activity is required for normal function of cells that require high levels of ATP, such as mitochondria-rich osteoclasts. The peptide hormone calcitonin, which inhibits osteoclast function, also down-regulates Cox activity. Increasing Src kinase activity prevented the inhibitory effect of calcitonin on Cox activity and osteoclast function. These results suggest that c-Src plays a previously unrecognized role in maintaining cellular energy stores by activating Cox in mitochondria.

Introduction

The nonreceptor tyrosine kinase c-Src, which is highly conserved throughout evolution and widely expressed, is a member of a family of nine protein tyrosine kinases that associate with the cytoplasmic surface of cellular membranes (Brown and Cooper, 1996). It is generally thought that Src's regulation of cell adhesion, movement, and proliferation involves its activity as a plasma membrane–associated molecular switch that links a variety of extracellular cues to specific intracellular signaling pathways (Thomas and Brugge, 1997). c-Src has also been reported to be present on late endosomes in fibroblasts (Kaplan et al., 1992), synaptic vesicles in PC12 cells (Linstedt et al., 1992), secretory vesicles in chromaffin cells (Grandori and Hanafusa, 1988), vesicular structures in osteoclasts (Horne et al., 1992; Tanaka et al., 1996), and the Golgi apparatus in CHO cells (Bard et al., 2002). More recently, Lyn, another Src family kinase, was found in rat brain mitochondria (Salvi et al., 2002). However, the functions of c-Src on intracellular membranes still remain to be determined.

In aerobic conditions, most of the energy produced by eukaryotic cells is in the form of ATP generated by mitochondrial oxidative phosphorylation, a process in which electrons are passed along a series of carrier molecules called the electron transport chain. These electrons are initially generated from NADH and $FADH_2$, which are produced by the metabolism of nutrients such as glucose, and are ultimately transferred to molecular oxygen. The electron transport chain consists of four respiratory enzyme complexes. Cytochrome *c* oxidase (Cox),* which contains 13 subunits, is the terminal oxidase of cell respiration. The three major subunits of Cox are encoded by mitochondrial DNA and form the functional core of the enzyme; this core is surrounded by 10 nuclear-coded small subunits. Cox reduces dioxygen to water with four electrons from cytochrome *c* and four protons taken up from the mitochondrial matrix, without the formation of reactive oxygen species. The energy generated by the passage of electrons down the electron transport chain creates a proton gradient across the membrane that drives ATP synthase to make ATP from ADP. The synthesized ATP is used for energy-requiring reactions in the matrix, and is exported to the cytosol by the adenine nucleotide translocator in exchange for cytosolic ADP (Wallace, 1999; van den Heuvel and Smeitink, 2001). Although osteoclasts contain large numbers of mitochondria, the regulation of their functioning has not been characterized.

Address correspondence to Roland Baron, Dept. of Orthopaedics and Rehabilitation, Yale University School of Medicine, PO Box 208044, New Haven, CT 06520-8044. Tel.: (203) 785-5986. Fax: (203) 785-2744. E-mail: roland.baron@yale.edu

Key words: oxidative phosphorylation; mitochondria; calcitonin; bone resorption; apoptosis

*Abbreviations used in this paper: Cox, cytochrome *c* oxidase; Csk, COOH-terminal Src family kinase; CT, calcitonin; ERK, extracellular signal-regulated kinase; MEK, MAPK/ERK kinase; MOI, multiplicity of infection; OCL, osteoclast-like cell; TRAP, tartrate-resistant acid phosphatase.

The Journal of Cell Biology, Volume 160, Number 5, March 3, 2003 709–718
http://www.jcb.org/cgi/doi/10.1083/jcb.200209098

Here, we show that c-Src is located within mitochondria and that it modulates Cox. Using mitochondria-rich osteoclasts as a model system, we investigated the physiological significance of the regulation of Cox by c-Src and found that Src-induced Cox activity is important for normal function of osteoclasts.

Results

c-Src is associated with mitochondria

Recently, Lyn, another Src family kinase, was found in rat brain mitochondria (Salvi et al., 2002). To examine whether or not c-Src is also located in mitochondria, organelles from HEK 293 cells were separated by ultracentrifugation on OptiPrep™ discontinuous gradients. The fractions were Western blotted using anti-Src and organelle-specific antibodies, including anti-Golgi 58K protein (Golgi complex), anti-EEA1 (early endosome), anti-calnexin (ER), anti-cathepsin D (lysosome), and anti-Cox subunit Vb (CoxVb; mitochondria; Fig. 1 A). A plasma membrane marker, PMCA (plasma membrane Ca^{2+} ATPase), was found in the lighter fractions 1–3. The Golgi complex and early endosomes had a wide range of distribution, in fractions 1–5 and 2–7, respectively. ER and lysosomes were found in fractions 3–6 and 6–8, respectively. Mitochondria were mainly in the more dense fractions 8–9. Src was detected in all fractions, suggesting that it associates with various intracellular membranes, including mitochondria.

To examine whether Src is located inside or outside the mitochondria, we next assessed the sensitivity of the mitochondria-associated Src to proteinase K. For this experiment, the freshly prepared mitochondrial fraction was incubated with proteinase K in the absence or presence of Triton X-100, and the mitochondrial proteins were Western blotted for Src, Bcl-2, and CoxVb. As shown in Fig. 1 B, CoxVb, which is located inside the mitochondria, was fully protected from proteinase K in the absence of detergent, whereas Bcl-2, which is associated with the external mitochondrial membrane, was completely degraded regardless of whether Triton X-100 was present or not. Interestingly, a significant fraction of Src was not degraded by proteinase K in the absence of Triton X-100, suggesting that some Src is located inside the mitochondria.

To confirm these biochemical results, we used immunoelectron microscopy to directly visualize c-Src in mitochondria. As shown in Fig. 1 C, c-Src was associated with the inner mitochondrial membrane. As positive control, we used an antibody against the membrane-bound Cox subunit IV (CoxIV). In contrast, no mitochondria showed labeling in the absence of the c-Src antibody (negative control).

To further confirm the specificity of the immunogold labeling, we used mitochondria-enriched preparations from c-$Src^{+/?}$ and c-$Src^{-/-}$ osteoclast-like cells (OCLs). As shown in Fig. 1 D, c-Src was also located inside mitochondria of c-$Src^{+/?}$ OCLs, whereas no labeling was seen in the mitochondria of c-$Src^{-/-}$ OCLs.

c-Src phosphorylates Cox

Mitochondria were isolated from c-Src–overexpressing HEK 293 cells, and the mitochondrial proteins were separated on two-dimensional nondenaturing/denaturing gels (2-D gels). Western blots of the mitochondrial proteins suggested that one of the tyrosine-phosphorylated mitochondrial proteins was the Cox subunit II (CoxII; Fig. 2 A). To determine directly whether Src can phosphorylate CoxII, immunoprecipitated CoxII and the total mitochondrial fraction (MT) were Western blotted with anti-phosphotyrosine and anti-CoxII antibodies. Transfection of cells with c-Src resulted in increased tyrosine phosphorylation of CoxII (Fig. 2 B). Src could be phosphorylating CoxII directly, or it could be acting indirectly through Src-activated pathways involving other kinase(s). To distinguish between these two possibilities, in vitro kinase assays were performed using purified c-Src and CoxII. Immunoprecipitated CoxII was incubated

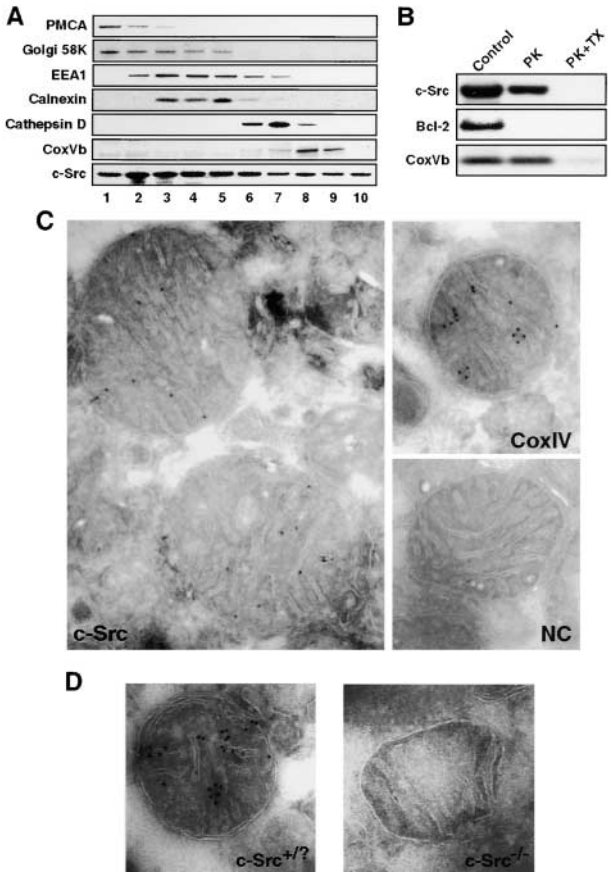

Figure 1. **c-Src localization in subcellular fractions and purified mitochondria.** (A) Subcellular fractionation of homogenized HEK 293 cells. Cell membranes were fractionated by centrifugation on discontinuous OptiPrep™ gradients, and the resulting fractions were immunoblotted with anti-PMCA, anti-Golgi 58K, anti-EEA1, anti-calnexin, anti-cathepsin D, anti-CoxVb, and anti-Src antibodies. (B) The mitochondrial fraction was isolated as described in Materials and methods and treated with 50 ng/ml proteinase K (PK) in the absence or presence of 0.5% Triton X-100 (TX) at RT for 30 min. The reaction was analyzed by Western blotting using antibodies to c-Src, Bcl-2, and CoxVb. (C) Immunogold labeling of c-Src in isolated mitochondria from HEK 293 cells. As positive control, CoxIV antibody was used for the primary antibody. As negative control (NC), gold-labeled secondary antibody was applied in the absence of c-Src antibody. (D) Immunogold labeling of c-Src in isolated mitochondria from c-$Src^{+/?}$ and c-$Src^{-/-}$ OCLs. c-Src was associated with the inner mitochondrial membrane in c-$Src^{+/?}$ OCLs, whereas no labeling was detected in the mitochondria of c-$Src^{-/-}$ OCLs.

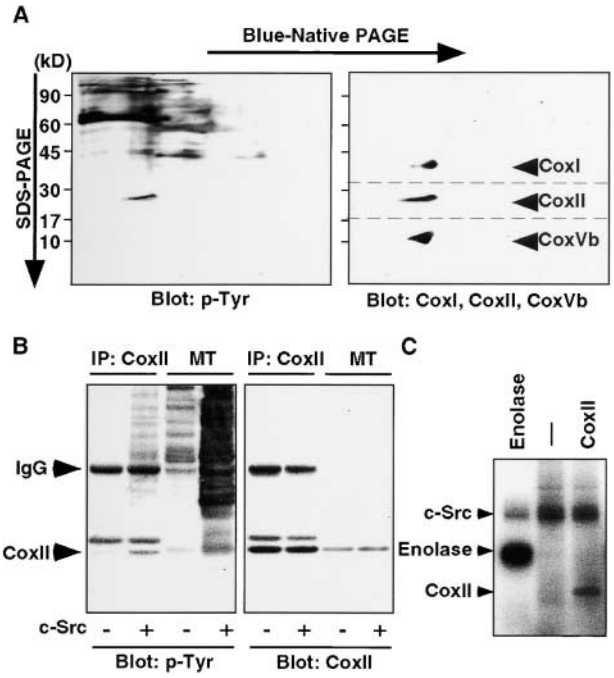

Figure 2. **Phosphorylation of Cox by c-Src.** (A) Immunodetection of phosphotyrosine and Cox subunits in mitochondria from c-Src–overexpressing HEK 293 cells analyzed by two-dimensional electrophoresis. Mitochondrial proteins were separated in the first dimension by nondenaturing Blue-native PAGE and in the second dimension by SDS-PAGE, and were then transferred to nitrocellulose membranes. Membranes were immunoblotted with anti-phosphotyrosine (p-Tyr) antibody, then stripped, cut in three parts at the dotted lines, and reprobed with antibody to Cox subunits. The position of CoxI, CoxII, and CoxVb are indicated on the right. (B) Tyrosine phosphorylation of CoxII in HEK 293 cells with or without transfected c-Src expression vector. Endogenous CoxII protein was immunoprecipitated, and Western blotting was performed with anti-phosphotyrosine antibody. The membrane was then reprobed with anti-CoxII antibody. MT, total mitochondrial fraction. (C) Enolase and CoxII were incubated with c-Src in kinase buffer containing $\gamma[^{32}P]$ATP at 30°C for 20 min. Positions of c-Src, enolase, and CoxII are indicated on the left.

with purified c-Src in kinase buffer containing $\gamma[^{32}P]$ATP. Enolase was used as a positive control. The reaction was subjected to SDS-PAGE and the phosphorylation analyzed by autoradiography. The results (Fig. 2 C) showed that c-Src could phosphorylate CoxII directly.

Cox activity is down-regulated by c-Src deficiency

To examine the functional consequences of the tyrosine phosphorylation of Cox by Src, we investigated whether or not Src kinase activity affected Cox activity. For this purpose, we used Src family tyrosine kinase–deficient mouse embryonic fibroblasts (Klinghoffer et al., 1999). As shown in Fig. 3 A, Cox activity in $Src^{-/-}$ $Yes^{-/-}$ $Fyn^{-/-}$ cells (SYF) was significantly decreased compared with $Yes^{-/-}$ $Fyn^{-/-}$ cells (Src++). Furthermore, reintroduction of c-Src into SYF cells (c-Src) restored Cox activity to the higher level of Src++ cells (Fig. 3 A). In contrast, there was no significant difference of complex I (NADH:ubiquinone oxidoreductase) activity among these cell types (Fig. 3 B). These results suggest that Src promotes Cox activity in mouse embryonic fibroblasts.

If c-Src promotes Cox activity under physiological conditions, one would predict that Cox activity would be lower in mitochondria from $c\text{-}Src^{-/-}$ animals. Therefore, we isolated mitochondria from several tissues of $c\text{-}Src^{+/?}$ and $c\text{-}Src^{-/-}$ mice (liver, kidney, and muscle) and assayed Cox activity. As shown in Fig. 3 C, Cox activity in mitochondria from liver and kidney were significantly decreased when Src was absent. In contrast, there was little difference in mitochondria from muscle, possibly due to relatively lower levels of expression of c-Src or to complete compensation by other Src family members.

Cox activity is positively correlated with c-Src kinase activity

To examine the physiological significance of the up-regulation of Cox by Src, we selected osteoclasts as a model system. Osteoclasts, the multinucleated giant cells responsible for bone resorption, have large numbers of mitochondria and express high levels of c-Src (Horne et al., 1992; Tanaka et al., 1992; Baron et al., 1993), and high levels of ATP are re-

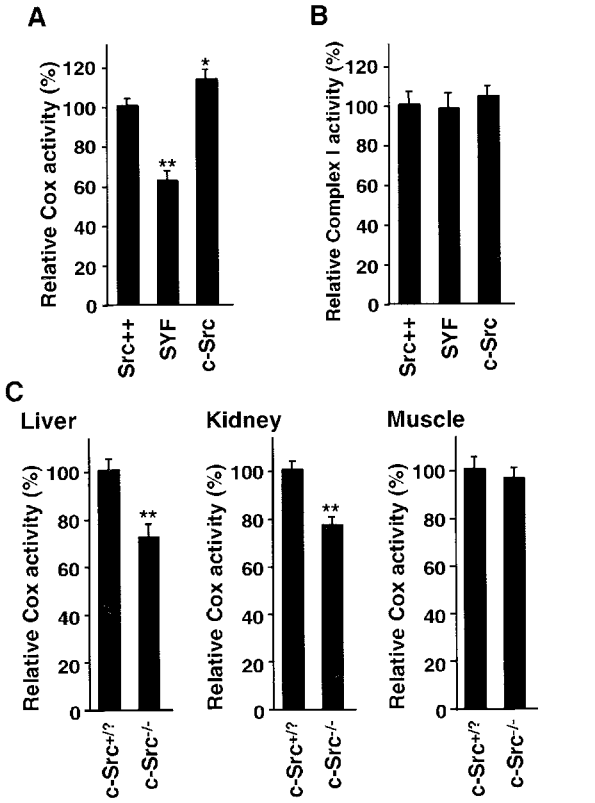

Figure 3. **Cox activity in c-Src–deficient cells.** (A) Cox activity in cells expressing endogenous Src (Src++), SYF cells (SYF), and SYF cells transfected with c-Src (c-Src) was measured by determining the increase in OD (450 nm) as described in Materials and methods. The values are means ± SD ($n = 8$; *, $P < 0.05$ compared with Src++ cells; **, $P < 0.01$). (B) Complex I (NADH:ubiquinone oxidoreductase) activity in cells expressing endogenous Src (Src++), SYF cells (SYF), and SYF cells transfected with c-Src (c-Src). No significant difference was found. The values are means ± SD ($n = 8$). (C) Cox activity of liver, kidney, and muscle in $c\text{-}Src^{+/?}$ and $c\text{-}Src^{-/-}$ mice. The values are means ± SD ($n = 8$; **, $P < 0.01$ compared with $c\text{-}Src^{+/?}$ OCLs).

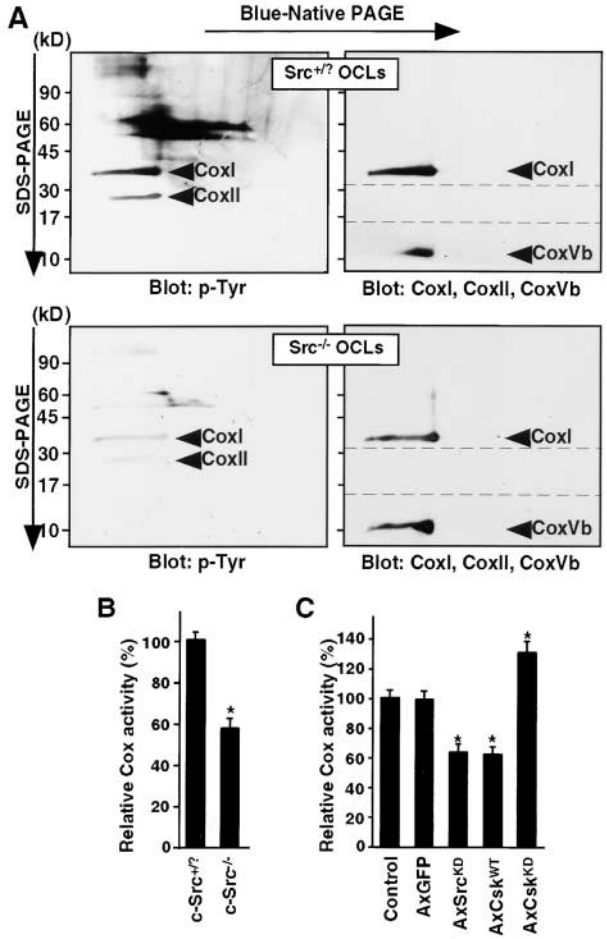

Figure 4. **c-Src kinase activity modulates Cox activity in osteoclasts.** (A) Immunodetection of phosphotyrosine and Cox subunits in mitochondria from c-Src$^{+/?}$ and c-Src$^{-/-}$ OCLs analyzed by two-dimensional electrophoresis. Membranes were immunoblotted with anti-phosphotyrosine (p-Tyr) antibody, then stripped, cut in three parts at the dotted lines, and reprobed with antibody to Cox subunits. Although the CoxII antibody did not recognize mouse CoxII, we can identify CoxII in the 2-D gel by its relative mobility. The position of CoxI, CoxII, and CoxVb are indicated. (B) Cox activity in c-Src$^{+/?}$ and c-Src$^{-/-}$ OCLs. The values are means ± SD ($n = 8$; *, $P < 0.01$ compared with uninfected OCLs). (C) Cox activity in OCLs infected with AxGFP, AxSrc^{KD}, AxCsk^{WT}, or AxCsk^{KD} at an MOI of 100. The values are means ± SD ($n = 8$; *, $P < 0.01$ compared with uninfected OCLs).

quired to support acid secretion by the osteoclast V-ATPase as well as other functions that are required for bone resorption (Baron et al., 1993).

Two-dimensional gel analysis showed that CoxII in the mitochondria from the murine c-Src$^{+/?}$ OCLs was tyrosine-phosphorylated as had been observed in the mitochondria from the human cell line. Interestingly, CoxI was also tyrosine-phosphorylated. Much less tyrosine phosphorylation of these proteins was observed in mitochondria from c-Src$^{-/-}$ OCLs (Fig. 4 A), although the low level of residual tyrosine phosphorylation suggests that other Src family tyrosine kinase may also phosphorylate Cox subunits.

Cox activity was reduced in c-Src$^{-/-}$ OCLs formed in vitro (Fig. 4 B), as it had been in fibroblasts that lack multiple the Src family tyrosine kinases and in the liver and kidney from the c-Src$^{-/-}$ mice, further indicating that Src regulates Cox activity. To test whether modulating Src kinase activity in OCLs would affect Cox activity and cell function (i.e., bone resorption), we used adenovirus vectors containing kinase-dead c-Src (AxSrc^{KD}), wild-type COOH-terminal Src family kinase (AxCsk^{WT}), or kinase-dead Csk (AxCsk^{KD}). Wild-type Csk phosphorylates the negative regulatory site (Tyr-527) of c-Src (Nada et al., 1991), inhibiting Src activity. Conversely, Csk^{KD} acts as a dominant-negative molecule against endogenous Csk, increasing Src kinase activity and bone-resorbing activity in osteoclasts (Miyazaki et al., 2000a). As predicted, down-regulation of Src kinase activity by Src^{KD} or Csk^{WT} overexpression inhibited Cox activity in OCLs, whereas up-regulation of Src kinase activity by AxCsk^{KD} infection induced higher Cox activity (Fig. 4 C). Thus, Cox activity was positively correlated with Src kinase activity.

Cox activity contributes to osteoclast function

To determine if reducing Cox activity affects the bone-resorbing activity of OCLs, we took advantage of the fact that the nuclear-encoded Cox subunit IV (CoxIV) is absolutely required for Cox activity (Burke and Poyton, 1998). OCLs were infected with an adenovirus vector carrying CoxIV antisense (AxCoxIV^{AS}). The adenovirus vector that encodes GFP (AxGFP) was used as a control vector. The expression of CoxIV in OCLs infected with AxCoxIV^{AS} decreased in a multiplicity of infection (MOI)-dependent manner (Fig. 5 A). The decreasing levels of CoxIV correlated with decreased Cox activity in a biochemical assay; OCLs infected with AxCoxIV^{AS} at an MOI of 100 showed 45% of basal Cox activity (Fig. 5 B). As shown in Fig. 5 C, there was no significant change in Src kinase activity among OCLs infected with AxGFP or AxCoxIV^{AS}.

Osteoclasts adhere to the bone surface through specialized discrete structures in the clear zone called "podosomes," which are punctate structures containing short actin filaments and numerous associated proteins. The ring of podosomes, also referred to as the actin ring, is a characteristic of polarized osteoclasts. There was no morphological difference between uninfected OCLs and AxGFP-infected OCLs (unpublished data). As shown in the left panel of Fig. 5 D, tartrate-resistant acid phosphatase (TRAP)-stained OCLs infected with AxCoxIV^{AS} had an elongated shape rather than the typical rounded appearance of wild-type osteoclasts. To determine whether AxCoxIV^{AS} infection modulates the cytoskeletal organization of osteoclasts, F-actin was stained with rhodamine-conjugated phalloidin (Fig. 5 D). An actin ring was observed in >85% of the AxGFP-infected OCLs, whereas only 15% of OCLs infected with AxCoxIV^{AS} formed these rings. Consistent with the absence of the actin ring, bone-resorbing activity was progressively and severely inhibited as the MOI of AxCoxIV^{AS} increased (Fig. 5 E). Thus, basal Cox activity is required for normal bone resorption, consistent with the high ATP requirement of the V-ATPase and other ATP-dependent activities of resorbing osteoclasts. The inhibitory effect of AxCoxIV^{AS} on bone resorption was not reversed by Csk^{KD} overexpression (Fig. 5 G), even though c-Src kinase activity was increased in OCLs coinfected with AxCoxIV^{AS} and AxCsk^{KD} as much as it was

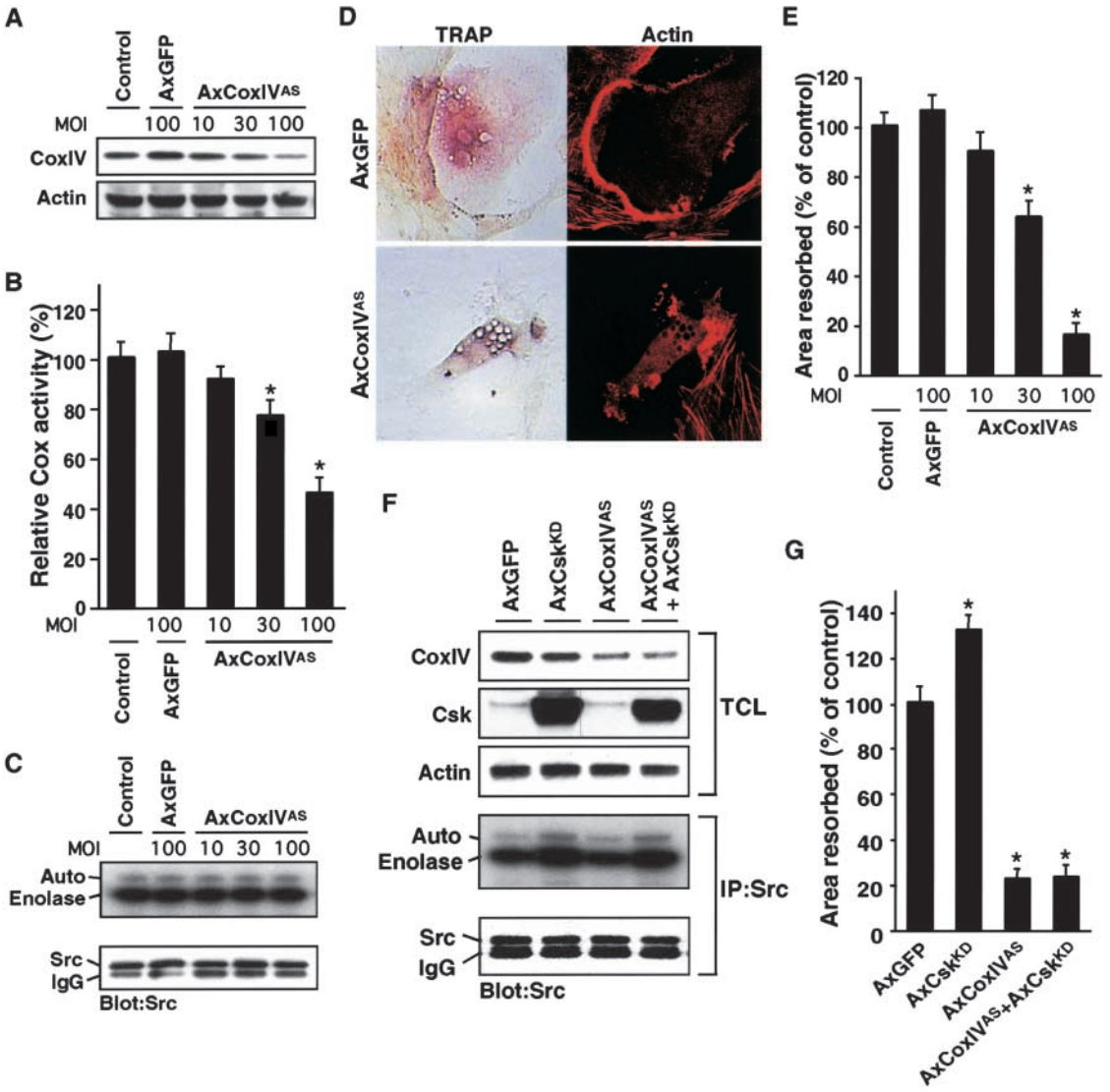

Figure 5. **CoxIV antisense prevents bone resorption in a dose-dependent manner.** (A) OCLs were infected with AxGFP or AxCoxIV^{AS} at the indicated MOIs. Membranes were immunoblotted with anti-CoxIV antibody, then stripped and reprobed with anti-actin antibody. (B) Cox activity in OCLs infected with AxGFP or AxCoxIV^{AS} at the indicated MOIs. Cox activity of the cells was measured as described in Materials and methods. The values are means ± SD ($n = 8$; *, $P < 0.01$ compared with uninfected OCLs). (C) c-Src kinase activity in OCLs infected with AxGFP or AxCoxIV^{AS} at the indicated MOIs was assayed by in vitro kinase assay using enolase as a substrate. (D) Effects of AxCoxIV^{AS} on osteoclast morphology. Co-cultures infected with AxGFP or AxCoxIV^{AS} at an MOI of 100 were plated on serum-coated glass coverslips for 12 h and then costained for TRAP activity (left) and for F-actin using rhodamine phalloidin (right). (E) Dentine-resorbing activity of OCLs expressing CoxIV antisense (AxCoxIV^{AS}). An aliquot of the OCL preparation was transferred to dentine and cultured for an additional 12 h. The resorbed area on the dentine slices was measured as described in Materials and methods. The values are means ± SD ($n = 8$; *, $P < 0.01$ compared with uninfected OCLs). (F) OCLs infected with both AxCsk^{KD} and AxCoxIV^{AS} expressed Csk and CoxIV at levels similar to those of the cells infected with either AxCsk^{KD} or AxCoxIV^{AS} alone. c-Src kinase activity in OCLs coinfected with AxCsk^{KD} and AxCoxIV^{AS} was measured by in vitro kinase assay using enolase as a substrate. (G) Dentine-resorbing activity of OCLs coinfected with AxCsk^{KD} and AxCoxIV^{AS}. An aliquot of the OCL preparation was transferred onto dentine and cultured for an additional 12 h. The values are means ± SD ($n = 8$; *, $P < 0.01$ compared with AxGFP-infected OCLs).

in OCLs infected with AxCsk^{KD} alone (Fig. 5 F). Together, these results indicate that Cox is a downstream effector of Src and that it is required in order for osteoclast function to proceed normally.

Down-regulation of Cox activity does not affect the survival of OCLs

Inhibition of Cox can lead to the release of cytochrome *c* from mitochondria into the cytoplasm (Yang et al., 1998), which in turn activates a signaling cascade that ultimately cleaves and activates caspase-3, causing apoptosis (Liu et al., 1996; Kluck et al., 1997; Li et al., 1997). Therefore, it is possible that the CoxIV^{AS}-induced decrease in Cox activity increased OCL apoptosis, with accompanying disorganization of the cytoskeleton and decreased bone-resorbing activity. To address this question, we used a nucleic acid stain to visualize the morphology of nuclei. The nuclei of OCLs infected with AxCoxIV^{AS} were stained uniformly with TO-

PRO®-3 (Fig. 6 A), suggesting that the disruption of cytoskeleton by AxCoxIV^{AS} was not due to apoptosis. Next, we investigated the survival of AxCoxIV^{AS}-infected OCLs, both in the presence of osteoblastic cells, which promote OCL survival by secreting M-CSF, RANK ligand, and other factors, and in their absence, where OCLs become apoptotic and die within 24 h. There was no significant difference in the survival of AxGFP-infected OCLs and AxCoxIV^{AS}-infected OCLs either in the presence of osteoblastic cells (unpublished data) or in their absence (Fig. 6 D). Thus, reducing Cox activity to less than half of the normal level (Fig. 5 B) does not affect osteoclast survival under either condition, and the CoxIV^{AS}-induced changes in cytoskeletal organization and decreased bone-resorbing activity are not due to increased apoptosis.

Previously, we have reported that extracellular signal–related kinase (ERK) activation by constitutively active MAPK/ERK kinase 1 (MEK^{CA}) expression strongly promotes osteoclast survival (Miyazaki et al., 2000b). Therefore, we investigated the survival of OCLs coinfected with AxCoxIV^{AS} and AxMEK^{CA}, which expressed CoxIV and MEK at levels similar to the cells infected with either AxCoxIV^{AS} or AxMEK^{CA} (Fig. 6 B). 18 h after purification, the level of proteolyzed caspase-3 had increased spontaneously in OCLs infected with AxGFP, and AxCoxIV^{AS} infection further increased the amount of the active caspase-3 subunit in OCLs (Fig. 6 C). The infection with AxMEK^{CA} markedly reduced the amount of active caspase-3 in both AxGFP- and AxCoxIV^{AS}-infected cells. Consistent with this result, the expression of MEK^{CA} promoted the survival of OCLs coinfected with AxCoxIV^{AS} (Fig. 6, D and E). The coinfected OCLs did not display the typical rounded appearance of mature osteoclasts (Fig. 6 E). These data further indicate that the down-regulation of osteoclast function by AxCoxIV^{AS} is mostly due to factors other than increased apoptosis.

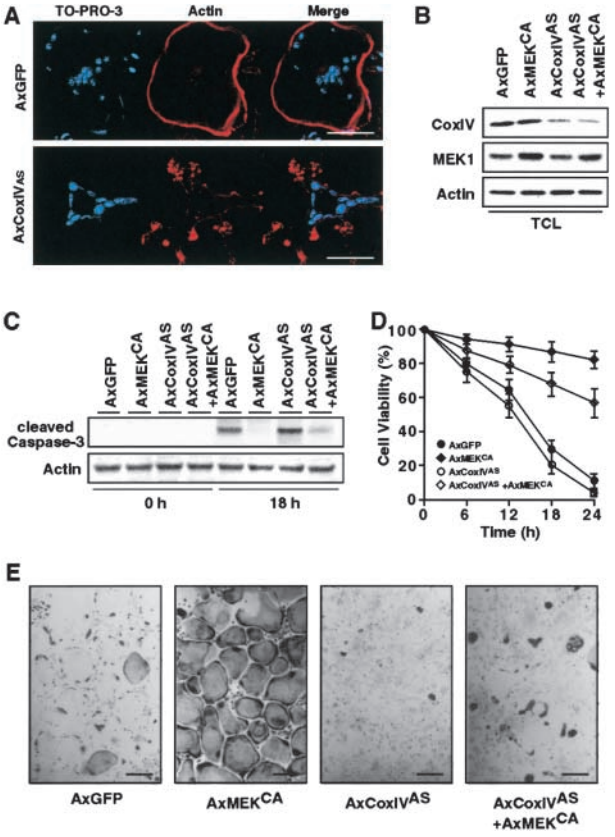

Figure 6. **Infection with AxCoxIV^{AS} does not affect OCL survival.** (A) Co-cultures infected with AxGFP or AxCoxIV^{AS} at an MOI of 100 were plated on serum-coated glass coverslips for 12 h and then stained for F-actin using rhodamine phalloidin (red). To visualize the nuclei of the OCLs, the cells were stained with TO-PRO®-3 (blue). Bars, 50 μm. (B) OCLs coinfected with AxMEK^{CA} and AxCoxIV^{AS} at MOIs of 100 expressed the proteins at levels similar to the levels in the cells infected with either AxMEK^{CA} or AxCOxIV^{AS} alone. (C) Caspase-3 cleavage in OCLs infected with AxMEK^{CA} and/or AxCoxIV^{AS}. The time-dependent change in cleaved caspase-3 in purified OCLs was detected by Western blotting with anti-cleaved caspase-3 antibody. (D) Survival of OCLs infected with AxMEK^{CA} or/and AxCoxIV^{AS}. After purification, infected OCLs were incubated with αMEM/10% FBS for the indicated times. The number of viable cells remaining at the different time points is shown as a percentage of the number of cells at time 0. (E) Typical TRAP staining of OCLs 24 h after purification in the experiment quantified in (D). Bars, 100 μm.

Calcitonin down-regulates Cox activity in OCLs

Calcitonin (CT) is a 32-amino acid polypeptide hormone that inhibits osteoclastic bone resorption in a cAMP-dependent manner (Nicholson et al., 1986). Because cAMP negatively regulates Cox activity (Yang et al., 1998), we investigated the effect of CT treatment on Cox activity in OCLs. As shown in Fig. 7 A, CT induced a decrease in Cox activity in OCLs, with the lowest level attained after 30 min of stimulation. In contrast, c-Src kinase activity remained unchanged after CT stimulation (Fig. 7 B). These results suggest that Cox, but not c-Src, may play a role in CT-induced inhibition of bone resorption.

Increasing c-Src kinase activity reverses the inhibitory effect of CT on bone resorption

Because c-Src kinase activity and CT treatment affect Cox activity in osteoclasts in opposite ways, we examined the interaction of c-Src and CT-induced signaling pathways in the regulation of Cox. c-Src kinase activity was increased by infecting OCLs with AxCsk^{KD}, and the effect of CT on Cox activity and bone resorption was determined. Up-regulation of Src kinase activity by AxCsk^{KD} reversed the CT-induced inhibition of OCL Cox activity (Fig. 7 D), whereas increasing Src kinase activity did not affect CT-induced cAMP production (Fig. 7 C). Similarly, the dose-dependent inhibition of the pit-forming activity by CT was largely prevented by Csk^{KD} overexpression. In the presence of 10^{-9} M CT, which almost completely inhibited pit formation by AxGFP-infected cells, the bone-resorbing activity of AxCsk^{KD}-infected OCLs was almost as great as that of untreated AxGFP-infected OCLs (Fig. 7 E). Csk^{KD} expression in OCLs also prevented the CT-induced disruption of actin rings (Fig. 7 F). More than 80% of Csk^{KD}-expressing OCLs still displayed the typical actin rings even after CT treatment, whereas the disruption of actin ring formation was observed in >80% of AxGFP-infected OCLs. Thus, c-Src antagonizes CT-induced inhibition of both Cox activity and bone resorption.

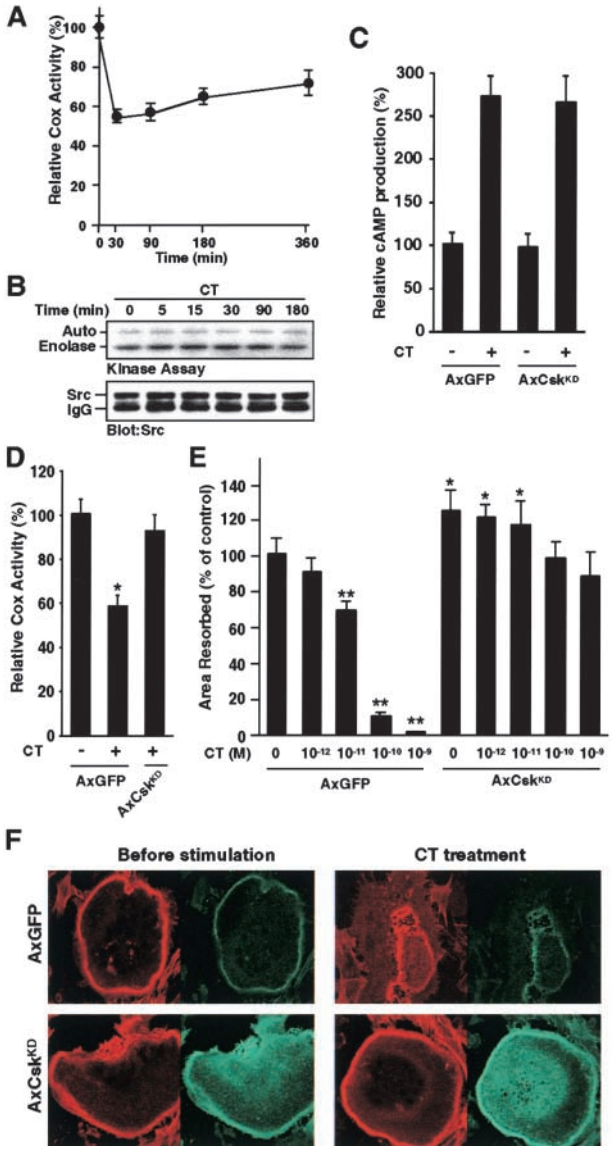

Figure 7. **The effects of CT treatment on OCLs.** (A) Change in Cox activity with time in OCLs treated with CT (10^{-9} M). Cox activity in OCLs at the different time points is shown as a percentage of that in the cells at time 0. (B) c-Src kinase activity in OCLs treated with CT (10^{-9} M) was measured by in vitro kinase assay using enolase as a substrate. (C) AxGFP- or AxCsk^{KD}-infected OCLs were incubated for 20 min in the presence or absence of CT (10^{-9} M). cAMP production by the cells was measured as described in Materials and methods ($n = 8$). There was no significant difference in CT-induced cAMP production by GFP-expressing and Csk^{KD}-expressing OCLs. (D) AxGFP- or AxCsk^{KD}-infected OCLs were incubated for 30 min in the presence or absence of CT (10^{-9} M). Cox activity of the cells was measured as described in Materials and methods ($n = 8$; *, $P < 0.01$ compared with untreated AxGFP-infected OCLs). (E) Purified OCLs infected with AxGFP or AxCsk^{KD} at an MOI of 100 were cultured on dentine for 12 h with increasing concentrations of CT. The values are means ± SD ($n = 8$; *, $P < 0.05$ compared with untreated AxGFP-infected OCLs; **, $P < 0.01$). (F) Double immunofluorescence staining of F-actin (red) and Csk (green) in OCLs infected with AxGFP or AxCsk^{KD} at an MOI of 100. Purified GFP- or Csk^{KD}-expressing OCLs were treated with or without CT (10^{-9} M) for 1 h. Csk^{KD} expression prevented CT-induced disruption of actin rings.

Discussion

The nonreceptor tyrosine kinase c-Src is a member of a family of nine protein tyrosine kinases that associate with the cytoplasmic surface of the cellular membrane (Brown and Cooper, 1996). Constitutively active mutants of Src are oncogenic, and study of these mutants has implicated c-Src in the control of cell growth and proliferation. However, c-Src is highly expressed in terminally differentiated cells such as platelets, neurons, and osteoclasts, indicating a physiological role for the protein unrelated to growth control. Targeted disruption of the c-*src* gene in mice induces osteopetrosis, a disorder characterized by decreased bone resorption, without showing any obvious morphological or functional abnormalities in other tissues or cells (Soriano et al., 1991). Osteoclasts, which are responsible for bone resorption, express high levels of c-Src protein, and c-Src–deficient osteoclasts have impaired ability to form the actin ring (Boyce et al., 1992). Together, these results indicate that c-Src plays an essential role in the normal cellular function of osteoclasts. c-Src is thought to be involved in intracellular signaling pathways mainly as a plasma membrane–associated molecular effector of a variety of extracellular stimuli. c-Src has also been reported to be present on some intracellular membranes including late endosomes, the Golgi apparatus, and vesicular structures (Grandori and Hanafusa, 1988; Horne et al., 1992; Kaplan et al., 1992; Linstedt et al., 1992; Tanaka et al., 1996; Bard et al., 2002). In this work, we found that c-Src is also located within mitochondria, where it appears to be associated with the inner membrane, indicating that c-Src is imported from the cytosol into mitochondria, not withstanding the absence of known mitochondrial import motifs in c-Src. Furthermore, several mitochondrial proteins were phosphorylated in c-Src–overexpressing HEK 293 cells and osteoclasts (Fig. 2 A and Fig. 4 A), suggesting that c-Src–catalyzed tyrosine phosphorylation of mitochondrial proteins, including Cox subunits, may regulates energy production by mitochondrial oxidative phosphorylation.

Our results support this hypothesis. c-Src deficiency results in decreased Cox activity in mouse embryonic fibroblasts, osteoclasts, and in several tissues. In addition, Cox activity was also correlated with c-Src kinase activity, decreasing when Src was down-regulated by the expression of Csk^{WT} or the dominant-negative Src^{KD}, and increasing when Src activity was up-regulated by the expression of Csk^{KD}. Furthermore, we found that Cox activity was required for normal actin ring formation and bone-resorbing activity of OCLs. Thus, normal osteoclast Cox activity is important for both actin ring formation and bone resorption. The disruption of the actin ring could itself explain the loss of bone-resorbing activity, although there are a number of other ATP-dependent events, especially those involved in cell motility, proton secretion, and the maintenance of electrochemical homeostasis, that are necessary for normal osteoclast function (Baron et al., 1993). The failure of any of these processes as a consequence of diminished ATP levels could contribute to the observed loss of bone resorption when Cox activity decreases. The fact that treating the cells with the classical Cox inhibitor KCN or with the complex I inhibitor rotenone or the complex III inhibitor myxothiazol

also decreased bone resorption (unpublished data) further demonstrates the sensitivity of osteoclasts to decreased oxidative phosphorylation.

Promoting Cox activity is clearly not the only role of c-Src that is important for osteoclast function. For example, we have previously reported that c-Src forms a complex with autophosphorylated Pyk2 on integrin stimulation (Sanjay et al., 2001). Preventing the Pyk2–SrcSH2 interaction by expressing Pyk2 with a mutated SrcSH2-binding site inhibited Src localization in adhesion structures, disrupted normal actin ring formation, and reduced the bone-resorbing activity of OCLs (unpublished data), suggesting that Pyk2-dependent recruitment of c-Src to adhesion structure of plasma membrane is also required for osteoclast function. Thus, it appears that c-Src plays several key roles in both mitochondria and plasma membrane–related functions that are critically important for osteoclast activity.

In addition, we found that CT treatment also regulates Cox activity in OCLs, but in a manner opposite that of c-Src, consistent with the report by Yang et al. (1998) that cAMP down-regulates Cox activity in CHO cells by inducing the dissociation of the PKA RIα regulatory subunit from the CoxVb. PKA has also been reported to either inhibit (Vang et al., 2001) or activate (Schmitt and Stork, 2002) c-Src, depending on the cells studied. However, we found in the present work that c-Src kinase activity in osteoclasts remained unchanged after CT treatment (Fig. 7 B). Thus, CT's effects on Cox activity, the osteoclast actin ring, and bone-resorbing activity are apparently not mediated by a change in c-Src activity, although the CT-induced inhibition of Cox and bone resorption were both reversed when c-Src activity was artificially increased by expressing the dominant-negative Csk^{KD}. Elucidating how CT and Src interact in regulating Cox activity and bone resorption generally remains a topic of future research.

In this work, we demonstrated that Cox activity is not important for osteoclast survival. In spite of decreased Cox activity and bone resorption, CT promotes osteoclast survival in vitro (Selander et al., 1996). The enhanced survival of CT-treated OCLs indicates that CT is activating specific signaling events that antagonize OCL apoptosis. Because we have previously reported that activating the Ras/ERK signaling pathway markedly inhibits the spontaneous apoptosis of OCLs (Miyazaki et al., 2000b), we examined the interaction of CT-induced signaling and the Ras/ERK cascade in regulating OCL survival. CT (10^{-9} M) stimulated a rapid and transient increase in ERK activity in OCLs (unpublished data). The expression of a dominant-negative Ras (Ras^{DN}) inhibited both basal ERK activity and the CT-induced activation of ERK in OCLs, and reversed the CT-induced increase in osteoclast survival (unpublished data), indicating that CT promotes osteoclast survival at least in part by activating ERK.

In the present paper, we showed that Src-induced Cox activity is involved in bone-resorbing activity of osteoclasts, but not in their survival. The pattern of responses to CT offers several interesting insights into the mechanisms that regulate osteoclast bone-resorbing activity and apoptosis. First, the fact that CT both inhibits bone resorption and protects against apoptosis clearly indicates that inhibition of bone resorption is not necessarily linked to apoptosis. It also provides further evidence of the importance of ERK in protecting osteoclasts from apoptosis because the CT-induced inhibition of Cox would be expected to promote apoptosis in the absence of the simultaneous induction of ERK activity. Consistent with the observation that CT protects osteoclasts against apoptosis, coexpression of constitutively active MEK1 and CoxIV antisense in OCLs promoted their survival (Fig. 6, D and E). Finally, the correlation between decreased bone resorption and decreased Cox activity together with decreased apoptosis provides strong evidence that Cox plays an important role in promoting bone resorption that is independent of protecting the cells against apoptosis.

Although CT is used therapeutically for diseases characterized by elevated bone resorption (i.e., osteoporosis, Paget's disease, and humoral hypercalcemia of malignancy), its mechanism of action is still largely unknown. Our demonstration that Cox activity is important for cytoskeletal organization and bone-resorbing activity of osteoclasts and that CT causes Cox activity to decrease identifies a novel response of the osteoclast to CT. This raises the possibility that the inhibitory effect of CT on bone resorption may be partly due to the down-regulation of Cox activity in mature osteoclasts.

The finding that Cox activity is modulated by c-Src reveals a new and potentially important aspect of Src's regulatory function. Upstream signaling elements could activate mitochondrial c-Src to increase ATP generation, thereby promoting cellular activity. The identification and characterization of signaling cascades that induce Src-mediated cellular metabolic activity present an interesting new avenue for further elucidating Src's role in regulating cell function.

Finally, the detection of c-Src (this paper) and Lyn (Salvi et al., 2002) within mitochondria, and our data indicating that c-Src phosphorylates and regulates Cox activity adds a hitherto unexpected element to our understanding of the regulation of bioenergetics. To our knowledge, this is the first evidence of the importation of tyrosine kinases into mitochondria or of a direct regulatory effect of tyrosine kinases on the electron transport chain. Thus, it constitutes a major change in the currently accepted paradigm of eukaryotic bioenergetics. The presence of Src family kinases in mitochondria is the first evidence that endosymbiants can acquire host-derived regulatory mechanisms during coevolution, and thus calls attention to a previously unappreciated aspect of the evolution of eukaryotic bioenergetics that merits further attention.

Materials and methods

Antibodies and chemicals

MEM, α modification (αMEM), DME, and FBS were purchased from GIBCO BRL. Collagen was obtained from Nitta Gelatin Co. Bacterial collagenase and dispase were purchased from Calbiochem. Mouse monoclonal anti-cathepsin D, anti-calnexin, anti-EEA1, anti-MEK1, and anti-Csk antibodies were obtained from BD Biosciences. Dr. T. Vanaman (University of Kentucky, Lexington, KY) provided anti-plasma membrane Ca^{2+} ATPase (PMCA; Dean et al., 1997; Chen et al., 2001). Mouse monoclonal anti-Src antibody (Ab-1) was purchased from Oncogene Research Products, anti-avian-Src antibody from Upstate Biotechnology, anti-Golgi 58K antibody from Sigma-Aldrich, anti-Bcl-2 antibody from Santa Cruz Biotechnology, Inc., and anti-CoxI, -CoxII, -CoxIV, and -CoxVb antibodies from Molecular

Probes, Inc. Anti-cleaved caspase-3 antibody was purchased from New England Biolabs, Inc. Both anti–mouse and anti–rabbit HRP-conjugated secondary antibodies were obtained from Fisher Scientific.

Cells and cell cultures

HEK 293 cells were cultured in αMEM/10% FBS. SYF, Src++, and c-Src cells were purchased from the American Type Culture Collection and cultured in DME/10% FBS. OCLs were obtained from coculture of osteoblastic cells and bone marrow cells in the presence of 10 nM 1α, 25 dihydroxy vitamin D_3 [1α,25$(OH)_2D_3$], and 1 μM prostaglandin E_2 [PGE_2]. For biochemical assays, OCLs were purified as reported elsewhere (Tanaka et al., 1998). In brief, the cocultured cells were washed with αMEM and treated with 5 ml of αMEM containing 0.1% collagenase and 0.2% dispase for 10 min to remove osteoblastic cells. The purity of OCLs and their precursors in the final preparation was >90%.

Constructs and gene transduction

Adenovirus vectors carrying Cox subunit IV antisense [$AxCoxIV^{AS}$] and kinase-dead c-Src [K295 to M, $AxSrc^{KD}$] were constructed as reported previously (He et al., 1998). The recombinant adenovirus vector carrying wild-type Csk [$AxCsk^{wt}$] or kinase-dead Csk [K222 to R, $AxCsk^{KD}$] genes were described previously (Miyazaki et al., 2000a). Infection of OCLs with adenovirus vectors was performed after the method described previously (Tanaka et al., 1998). In short, on d 4, when OCLs began to appear, mouse cocultures were incubated for 1 h at 37°C with a small amount of αMEM containing the recombinant adenoviruses at the desired MOI. Cells were then washed twice with PBS and further incubated with αMEM containing 10% FBS, 10 nM 1α, 25$(OH)_2D_3$, and 1 μM PGE_2 at 37°C. Experiments were performed 3 d after the infection.

Subcellular fractionation

Subcellular fractionation was performed using OptiPrep™ (Accurate Chemical and Scientific Corporation) and ultracentrifugation as described elsewhere (Wentz-Hunter et al., 2002). A discontinuous gradient was prepared using 30, 25, 20, 15, and 10% OptiPrep™ solution. The postnuclear supernatant was overlaid onto the discontinuous gradient and centrifuged at 100,000 *g* for 3 h at 4°C. The gradient was removed in 10 equal fractions collected from the top of the gradient.

Isolation of mitochondria

HEK 293 cells or purified OCLs were washed with PBS and resuspended in buffer A [20 mM Hepes, pH 8.0, 10 mM KCl, 1.5 mM $MgCl_2$, 1 mM EDTA, 250 mM sucrose, 1 mM PMSF, 10 μg/ml leupeptin, 10 μg/ml aprotinin, and 0.2 mM sodium orthovanadate] for 30 min on ice, and then Dounce homogenized. Unbroken cells and nuclei were pelleted by centrifugation at 1,500 *g* for 5 min. Supernatants were further centrifuged at 10,000 *g* for 30 min. Blue-native PAGE was performed as described previously (Schagger and von Jagow, 1991). The mitochondrial pellets were solubilized in 1.5 M ε-amino-n-caproic acid (Sigma-Aldrich), 50 mM Bistris/HCl, pH 7.0, and 10 μl of 10% n-dodecylmaltoside (Roche). Insoluble material was removed by centrifugation for 20 min at 20,000 *g*. The supernatant was supplemented with 5 μl of sample buffer (5% Serva Blue G in 750 mM ε-amino-*n*-caproic acid), and electrophoresed through 4 to 12% polyacrylamide gradient gels. Strips of the first-dimension gel containing separated protein complexes were cut out and incubated with 1% SDS and 1% 2-mercaptoethanol for 45 min at RT and subjected to Tricine/SDS-PAGE for separation in the second dimension.

Immunogold labeling

Mitochondria-enriched preparations were fixed in 8% PFA in 0.25 M Hepes, pH 7.4, for 4 d, washed in PBS, and pelleted in 10% fish skin gelatin. The gelatin-embedded pellets were infiltrated overnight with 2.3 M sucrose at 4°C and frozen in liquid nitrogen. Ultrathin cryosections were prepared using a microtome (Ultracut; Leica) with cryoattachment, and transferred to formvar/carbon-coated specimen grids. Sections were incubated in PBS and 1% fish skin gelatin containing rabbit polyclonal anti-Src antibody (N-16 or SRC2; 1:50 dilution; Santa Cruz Biotechnology, Inc.) or mouse monoclonal anti-CoxIV (1:50 dilution; Molecular Probes, Inc.). Controls were incubated in PBS without primary antibody. After PBS washes, antibody-labeled grids were incubated in rabbit anti–mouse antibody (1:50 dilution) for 30 min. After PBS washes, all sections were incubated with PBS and 1% fish skin gelatin containing 10 nm protein A gold conjugate (1:80 dilution; J. Slot, Utrecht, Holland) for 30 min, washed in PBS, postfixed in 1% glutaraldehyde, and contrasted with 1.8% methyl cellulose and 0.5% uranyl acetate. Sections were viewed and images were recorded with a transmission electron microscope (model 410; Philips).

Proteinase K treatment

The mitochondrial fraction was treated with 50 ng/ml proteinase K (Sigma-Aldrich) in buffer A without protease inhibitors in the absence or presence of 0.5% Triton X-100 at RT for 30 min. The reaction was stopped by the addition of 1 mM phenylmethylsulfonylfluoride, and was analyzed by Western blotting using antibodies to c-Src, Bcl-2, and CoxVb.

Measurement of enzyme activities

Cox activity was measured as described elsewhere (Chrzanowska-Lightowlers et al., 1993). Mitochondria-enriched fractions from mouse embryonic fibroblasts or purified OCLs were incubated with 0.01% saponin in water for 5 min at RT. 50 μl of mitochondria solution was transferred to 96-well plates and 100 μl of substrate medium was added to each well to give a final concentration of 4 mM 3,3′ DAB-tetrachloride, 100 μM reduced cytochrome *c*, and 2 μg/ml catalase in 100 mM Na phosphate, pH 7.0. 100 mg cytochrome *c* in 2.5 ml of 100 mM sodium phosphate, pH 7.0, was reduced by addition of 5 mg ascorbic acid using a preequilibrated G25 M Sephadex column. Immediately after addition of substrate medium, light absorbance at 450 nm was measured for 30 min, and the amount of protein on culture plates was quantified by the Bradford method. Cox activity of the cells was expressed as the OD increase normalized to the amount of protein. The difference between groups was statistically evaluated by ANOVA.

NADH:ubiquinone oxidoreductase (Complex I) activity was assayed in 10 mM Tris/HCl buffer (pH 7.4) containing 50 mM KCl, 1 mM EDTA, 100 μg/ml soybean L-α-phosphatidylcholine, 125 μM NADH (β-form), 2 mM KCN, and 300 nM antimycin A. Mitochondria were disrupted by freezing and thawing 2–3 times, and were then added to the assay mix. 40 μM decylubiquinone was added, and the rate of disappearance of NADH was monitored at 340 nm (Estornell et al., 1993; James et al., 1996). Complex I activity of the cells was expressed as the OD decrease normalized to the amount of protein.

In vitro kinase assay

Equal amounts of lysate protein (500 μg) were incubated with 2 μg anti-Src antibody (Ab-1) for 1 h at 4°C, and the immune complexes were recovered with protein G Sepharose (GIBCO BRL). The immune complexes were washed three times with washing buffer and three times with kinase buffer (20 mM Hepes-NaOH, pH 7.4, and 10 mM $MgCl_2$). To examine the kinase activity of c-Src, one half of the immunoprecipitated material was used for in vitro kinase assay, and the other half for Western blotting analysis to ensure that an equal amount of c-Src protein was recovered by immunoprecipitation. In vitro kinase activity was assayed as previously reported (Miyazaki et al., 2000a). In brief, the samples were resuspended in 60 μl kinase buffer with 5 μCi γ[^{32}P]ATP in the presence of 1 μg acid-treated enolase, then incubated for 20 min at 30°C. The reaction was stopped by adding 20 μl of 4× sample buffer (250 mM Tris-HCl, pH 6.8, 8 mM EDTA, 12% SDS, 500 mM 2-mercaptoethanol, 15% glycerol, and 0.01% bromophenol blue). Samples were then subjected to SDS-PAGE under reducing condition, followed by autoradiography.

Pit formation assay

Functionally active OCLs were formed in cocultures performed on collagen gel as described previously (Miyazaki et al., 2000b). In brief, primary osteoblastic cells and bone marrow cells were cocultured in the presence of 10 nM 1α, 25 $(OH)_2D_3$, and 1 μM PGE_2 on 6-cm culture dishes coated with 0.2% collagen gel matrix. 3 d after the infection, OCLs were recovered by digesting the collagen gel with 0.2% collagenase for 20 min at 37°C. Cells released from the dishes were collected by centrifugation at 250 *g* for 5 min and resuspended in 5 ml αMEM containing 10% FBS. An aliquot of the crude OCL preparation was transferred onto dentine slices and cultured for an additional 12 h. After 12 h of incubation, the medium was removed and 1 M NH_4OH was added to the wells for 5 min. Adherent cells were removed from the dentine slices by ultrasonication, and the resorption pits were visualized by staining for 2 min with 1% toluidine blue and 1% sodium borate in PBS. The resorbed area was measured using an image analysis system linked to a light microscope (Osteometrics). The difference between groups was statistically evaluated by ANOVA.

Survival of OCLs

OCL survival was measured as reported previously (Miyazaki et al., 2000b). OCLs were purified 3 d after the infection, and some of the cultures were subjected to TRAP staining. Cell viability/survival is expressed as morphologically intact TRAP-positive multinucleated cells. Other cultures were further incubated for the indicated times, and then the number of living OCLs was determined. The number of viable cells remaining at the different time points is shown as a percentage of the cells at time 0.

cAMP assay

AxGFP- or AxCsk^{KD}-infected OCLs were purified and incubated with 10^{-9} M CT for 20 min. The cells were then lysed and the cAMP was measured using cAMP Biotrak™ Enzyme Immunoassay System (Amersham Biosciences), according to the manufacturer's instructions.

We thank Y. Tanaka for assistance in making adenoviruses, A. Sanjay, A. Bruzzaniti, G. DeBlasi, and C. Itzstein for discussion, K. Ford for maintaining the mouse colony, and K. Uematsu and A. Miyazaki for consistent support.

This work was supported by National Institutes of Health grants DE-04724 and AR-42927 (to R. Baron).

Submitted: 20 September 2002
Revised: 21 January 2003
Accepted: 21 January 2003

References

Bard, F., U. Patel, J.B. Levy, W.C. Horne, and R. Baron. 2002. Molecular complexes that contain both c-Cbl and c-Src associate with Golgi membranes. *Eur. J. Cell Biol.* 81:26–35.

Baron, R., J.-H. Ravesloot, L. Neff, M. Chakraborty, D. Chatterjee, A. Lomri, and W. Horne. 1993. Cellular and molecular biology of the osteoclast. *In* Cellular and Molecular Biology of Bone. M. Noda, editor. Academic Press, San Diego. 445–495.

Boyce, B.F., T. Yoneda, C. Lowe, P. Soriano, and G.R. Mundy. 1992. Requirement of pp60c-src expression for osteoclasts to form ruffled borders and resorb bone in mice. *J. Clin. Invest.* 90:1622–1627.

Brown, M.T., and J.A. Cooper. 1996. Regulation, substrates and functions of src. *Biochim. Biophys. Acta.* 1287:121–149.

Burke, P.A., and R.O. Poyton. 1998. Structure/function of oxygen-regulated isoforms in cytochrome c oxidase. *J. Exp. Biol.* 201:1163–1175.

Chen, D., W. Xu, P. He, E.E. Medrano, and S.W. Whiteheart. 2001. Gaf-1, a gamma-SNAP-binding protein associated with the mitochondria. *J. Biol. Chem.* 276:13127–13135.

Chrzanowska-Lightowlers, Z.M., D.M. Turnbull, and R.N. Lightowlers. 1993. A microtiter plate assay for cytochrome c oxidase in permeabilized whole cells. *Anal. Biochem.* 214:45–49.

Dean, W.L., D. Chen, P.C. Brandt, and T.C. Vanaman. 1997. Regulation of platelet plasma membrane Ca^{2+}-ATPase by cAMP-dependent and tyrosine phosphorylation. *J. Biol. Chem.* 272:15113–15119.

Estornell, E., R. Fato, F. Pallotti, and G. Lenaz. 1993. Assay conditions for the mitochondrial NADH:coenzyme Q oxidoreductase. *FEBS Lett.* 332:127–131.

Grandori, C., and H. Hanafusa. 1988. p60$^{c\text{-}src}$ is complexed with a cellular protein in subcellular compartments involved in exocytosis. *J. Cell Biol.* 107:2125–2135.

He, T.C., S. Zhou, L.T. da Costa, J. Yu, K.W. Kinzler, and B. Vogelstein. 1998. A simplified system for generating recombinant adenoviruses. *Proc. Natl. Acad. Sci. USA.* 95:2509–2514.

Horne, W.C., L. Neff, D. Chatterjee, A. Lomri, J.B. Levy, and R. Baron. 1992. Osteoclasts express high levels of pp60$^{c\text{-}src}$ in association with intracellular membranes. *J. Cell Biol.* 119:1003–1013.

James, A.M., Y.H. Wei, C.Y. Pang, and M.P. Murphy. 1996. Altered mitochondrial function in fibroblasts containing MELAS or MERRF mitochondrial DNA mutations. *Biochem. J.* 318:401–407.

Kaplan, K.B., J.R. Swedlow, H.E. Varmus, and D.O. Morgan. 1992. Association of p60$^{c\text{-}src}$ with endosomal membranes in mammalian fibroblasts. *J. Cell Biol.* 118:321–333.

Klinghoffer, R.A., C. Sachsenmaier, J.A. Cooper, and P. Soriano. 1999. Src family kinases are required for integrin but not PDGFR signal transduction. *EMBO J.* 18:2459–2471.

Kluck, R.M., E. Bossy-Wetzel, D.R. Green, and D.D. Newmeyer. 1997. The release of cytochrome c from mitochondria: a primary site for Bcl-2 regulation of apoptosis. *Science.* 275:1132–1136.

Li, P., D. Nijhawan, I. Budihardjo, S.M. Srinivasula, M. Ahmad, E.S. Alnemri, and X. Wang. 1997. Cytochrome c and dATP-dependent formation of Apaf-1/caspase-9 complex initiates an apoptotic protease cascade. *Cell.* 91: 479–489.

Linstedt, A.D., M.L. Vetter, J.M. Bishop, and R.B. Kelly. 1992. Specific association of the proto-oncogene product pp60$^{c\text{-}src}$ with an intracellular organelle, the PC12 synaptic vesicle. *J. Cell Biol.* 117:1077–1084.

Liu, X., C.N. Kim, J. Yang, R. Jemmerson, and X. Wang. 1996. Induction of apoptotic program in cell-free extracts: requirement for dATP and cytochrome c. *Cell.* 86:147–157.

Miyazaki, T., H. Takayanagi, M. Isshiki, T. Takahashi, M. Okada, Y. Fukui, H. Oda, K. Nakamura, H. Hirai, T. Kurokawa, and S. Tanaka. 2000a. In vitro and in vivo suppression of osteoclast function by adenovirus vector-induced csk gene. *J. Bone Miner. Res.* 15:41–51.

Miyazaki, T., H. Katagiri, Y. Kanegae, H. Takayanagi, Y. Sawada, A. Yamamoto, M.P. Pando, T. Asano, I.M. Verma, H. Oda, et al. 2000b. Reciprocal role of ERK and NF-κB pathways in survival and activation of osteoclasts. *J. Cell Biol.* 148:333–342.

Nada, S., M. Okada, A. MacAuley, J.A. Cooper, and H. Nakagawa. 1991. Cloning of a complementary DNA for a protein-tyrosine kinase that specifically phosphorylates a negative regulatory site of p60$^{c\text{-}src}$. *Nature.* 351:69–72.

Nicholson, G.C., J.M. Moseley, P.M. Sexton, F.A. Mendelsohn, and T.J. Martin. 1986. Abundant calcitonin receptors in isolated rat osteoclasts. Biochemical and autoradiographic characterization. *J. Clin. Invest.* 78:355–360.

Salvi, M., A.M. Brunati, L. Bordin, N. La Rocca, G. Clari, and A. Toninello. 2002. Characterization and location of Src-dependent tyrosine phosphorylation in rat brain mitochondria. *Biochim. Biophys. Acta.* 1589:181–195.

Sanjay, A., A. Houghton, L. Neff, E. Didomenico, C. Bardelay, E. Antoine, J. Levy, J. Gailit, D. Bowtell, W.C. Horne, and R. Baron. 2001. Cbl associates with Pyk2 and Src to regulate Src kinase activity, $\alpha_v\beta_3$ integrin-mediated signaling, cell adhesion, and osteoclast motility. *J. Cell Biol.* 152:181–195.

Schagger, H., and G. von Jagow. 1991. Blue native electrophoresis for isolation of membrane protein complexes in enzymatically active form. *Anal. Biochem.* 199:223–231.

Schmitt, J.M., and P.J. Stork. 2002. PKA phosphorylation of Src mediates cAMP's inhibition of cell growth via Rap1. *Mol. Cell.* 9:85–94.

Selander, K.S., P.L. Harkonen, E. Valve, J. Monkkonen, R. Hannuniemi, and H.K. Vaananen. 1996. Calcitonin promotes osteoclast survival in vitro. *Mol. Cell. Endocrinol.* 122:119–129.

Soriano, P., C. Montgomery, R. Geske, and A. Bradley. 1991. Targeted disruption of the c-src proto-oncogene leads to osteopetrosis in mice. *Cell.* 64:693–702.

Tanaka, S., N. Takahashi, N. Udagawa, T. Sasaki, Y. Fukui, T. Kurokawa, and T. Suda. 1992. Osteoclasts express high levels of p60c-src, preferentially on ruffled border membranes. *FEBS Lett.* 313:85–89.

Tanaka, S., M. Amling, L. Neff, A. Peyman, E. Uhlmann, J.B. Levy, and R. Baron. 1996. c-Cbl is downstream of c-Src in a signalling pathway necessary for bone resorption. *Nature.* 383:528–531.

Tanaka, S., T. Takahashi, H. Takayanagi, T. Miyazaki, H. Oda, K. Nakamura, H. Hirai, and T. Kurokawa. 1998. Modulation of osteoclast function by adenovirus vector-induced epidermal growth factor receptor. *J. Bone Miner. Res.* 13:1714–1720.

Thomas, S.M., and J.S. Brugge. 1997. Cellular functions regulated by Src family kinases. *Annu. Rev. Cell Dev. Biol.* 13:513–609.

van den Heuvel, L., and J. Smeitink. 2001. The oxidative phosphorylation (OXPHOS) system: nuclear genes and human genetic diseases. *Bioessays.* 23: 518–525.

Vang, T., K.M. Torgersen, V. Sundvold, M. Saxena, F.O. Levy, B.S. Skalhegg, V. Hansson, T. Mustelin, and K. Tasken. 2001. Activation of the COOH-terminal Src kinase (Csk) by cAMP-dependent protein kinase inhibits signaling through the T cell receptor. *J. Exp. Med.* 193:497–507.

Wallace, D.C. 1999. Mitochondrial diseases in man and mouse. *Science.* 283: 1482–1488.

Wentz-Hunter, K., J. Ueda, N. Shimizu, and B.Y. Yue. 2002. Myocilin is associated with mitochondria in human trabecular meshwork cells. *J. Cell. Physiol.* 190:46–53.

Yang, W.L., L. Iacono, W.M. Tang, and K.V. Chin. 1998. Novel function of the regulatory subunit of protein kinase A: regulation of cytochrome c oxidase activity and cytochrome c release. *Biochemistry.* 37:14175–14180.